

Conformationally Constrained Phosphotyrosyl Mimetics Designed as Monomeric Src Homology 2 Domain Inhibitors

Terrence R. Burke, Jr.,^{*,†} Joseph J. Barchi, Jr.,[†] Clifford George,[‡] Gert Wolf,[§] Steven E. Shoelson,[§] and Xinjian Yan[†]

Laboratory of Medicinal Chemistry, Building 37, Room 5C06, Developmental Therapeutics Program, Division of Cancer Treatment, National Cancer Institute, National Institutes of Health, Bethesda, Maryland 20892, Laboratory for the Structure of Matter, Naval Research Laboratory, Washington, D.C. 20375, Joslin Diabetes Center & Department of Medicine, Harvard Medical School, Boston, Massachusetts 02215

Received November 11, 1994[⊗]

Inhibitors of specific src homology 2 (SH2) domain binding interactions could potentially afford new therapeutic approaches toward a variety of diseases, including several cancers. To date SH2 domain inhibitors have been confined to small phosphotyrosyl (pTyr)-containing peptides that appear to bind along the surface of SH2 domains with specific recognition features protruding into the protein. Among these protrusions is the pTyr residue itself, which is inserted into a well-formed binding pocket. In the present study monomeric pTyr mimetics were prepared having key aspects of their structure constrained to conformations of the bound pTyr residue observed in the previously reported X-ray structure of a pTyr-peptide bound to the Lck SH2 domain. The resulting constrained pTyr mimetics were examined for inhibitory potency in six SH2 domain constructs: Lck, Src, Grb2, and the C-terminal SH2 domains of PLC γ (PLC γ -C) and the p85 subunit of PI-3 kinase (p85-C), as well as the N-terminal SH2 domain of SH PTP2. Although inhibition constants were in the millimolar range, it was observed that capping pTyr as its *N* ^{α} -acetyl carboxamide [(L)-1] provided a roughly 2–3-fold increase in potency relative to free pTyr. Diastereomeric indanylglycine-based analogues (\pm)-**3a,b** were essentially inactive. Of note was methanobenzazocine (\pm)-**2**. While being racemic and a partial pTyr structure, this analogue retained full binding potency of the enantiomerically pure *N* ^{α} -acetyl pTyr amide (L)-1. Modification and elaboration of **2** could potentially result in small molecule inhibitors having greater potency.

Protein-tyrosine kinases (PTKs) are critical mediators of normal and pathogenic cellular signaling that afford new targets for the development of therapeutic agents.¹ At the foundation of PTK-dependent signaling is the PTK-catalyzed phosphorylation of tyrosyl residues in target proteins with subsequent binding of secondary signaling molecules to the newly generated phosphotyrosyl (pTyr) sites. This pTyr-dependent binding is mediated by src homology 2 (SH2) domains contained within the binding protein. SH2 domains are homologous motifs of approximately 100 amino acids, which recognize and bind to pTyr-containing sequences.² The binding of SH2 domains to pTyr-containing proteins is so central to PTK signaling that PTK pathways could be interrupted by directing inhibitors either at the phosphorylation step (PTK catalytic site-directed agents) or at the SH2 binding interactions (SH2 domain-directed agents).^{3,4}

Development of SH2-directed agents is particularly appealing to the medicinal chemist for conceptual and practical reasons. Binding interactions are of high affinity, yet with rapid dissociation rates, potentially allowing effective binding competition between inhibitors and larger protein ligands.⁵ Since a significant portion of binding recognition occurs within a confined region surrounding the target pTyr residue, small 5–6-amino acid pTyr peptides can bind with high affinity, allowing them to effectively compete with larger peptide

and protein ligands for binding to SH2 domains. Additionally, because different SH2 domains recognize specific phosphopeptide sequences, pTyr peptides of various sequences are able to discriminate between SH2 domains in a sequence-dependent manner,⁶ thereby providing a basis for the development of inhibitors which are specific for select SH2 domains.

Design of SH2-directed inhibitors is facilitated by the fact that both NMR and X-ray structures have been solved for a variety of SH2 domains, including those with bound high-affinity phosphopeptide ligands.^{7–15} To date, all SH2 domains exhibit highly homologous tertiary structures, with binding to pTyr-containing peptides occurring in somewhat similar fashions.^{16,17} A well-defined binding pocket is observed for the pTyr residue, with secondary binding regions being observed for amino acids located from one to four residues C-terminal of the pTyr. This secondary binding provides much of the basis for sequence-dependent specificity of peptide and protein ligands. Among Src family SH2 domains, significant secondary binding occurs in a well-formed hydrophobic pocket, making the interaction of Src family SH2 domains with their pTyr peptides analogous to a two-pronged plug (pTyr-peptide) fitting into a two-hole socket.^{10,11} Other SH2 domains not in the Src family have been shown to exhibit secondary binding distributed over a wider area.^{14,15}

The development of SH2 inhibitors can be approached taking as a starting point the structures of 5–6-amino acid pTyr-containing peptides known to bind to target SH2 domains. In these peptides tyrosyl phosphorylation provides the essential recognition feature which

^{*} Laboratory of Medicinal Chemistry, NCI.

[†] Naval Research Laboratory.

[‡] Joslin Diabetes Center.

[⊗] Abstract published in *Advance ACS Abstracts*, March 15, 1995.

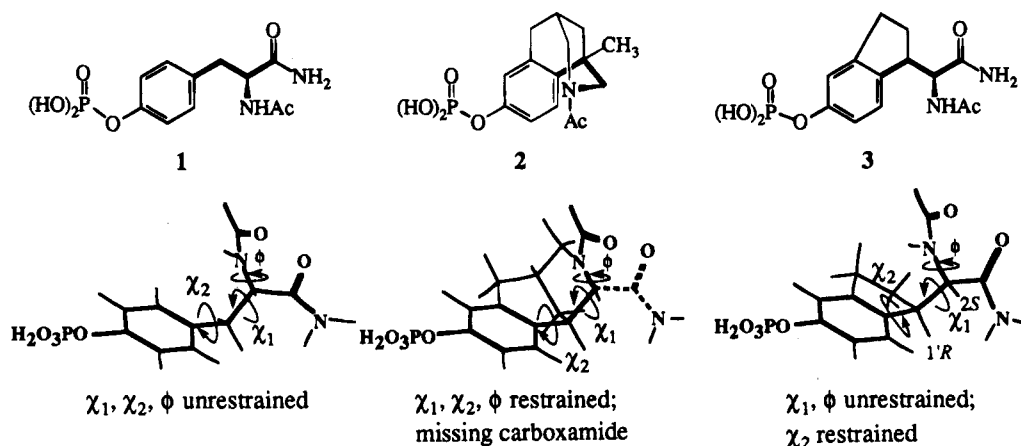


Figure 1. Structures of phosphotyrosyl mimetics 1–3 showing effects of rotational constraints on χ and ϕ torsion angles. The three-dimensional conformation of 1 is that displayed by the pTyr residue bound within the p56^{lck} SH2 domain as part of the high-affinity phosphopeptide E-P-Q-pY-E-E-I-P-I-Y-L.

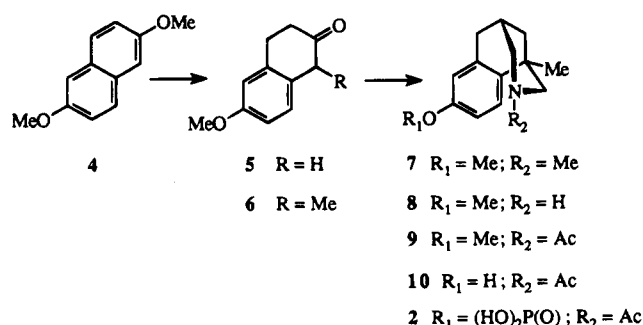
imparts high SH2 domain binding affinity to otherwise inactive peptides. The three-dimensional structures of pTyr-containing peptides complexed with SH2 domains demonstrate that the phosphate group is tightly bound within its binding pocket by multiple ionic and hydrogen bonds, while the remainder of the tyrosyl residue is held in place by additional hydrophobic and hydrogen-bonding interactions.^{9–15} In light of the critical nature of pTyr in the binding of pTyr-containing peptides through SH2 domain interactions, we wondered if small, amino acid-size agents designed specifically for high-affinity binding at the pTyr site could compete effectively with larger pTyr-containing peptides for binding to SH2 domains. Such small monomeric inhibitors could provide therapeutic advantages over larger peptide-based agents.

Using the X-ray structure of a high-affinity pTyr-containing peptide bound to the p56^{lck} SH2 domain,¹⁰ we were able to define both the conformation of the bound pTyr residue and the important hydrogen-bonding interactions. On the basis of the traditional approach which dictates that constraining the pTyr residue to its bound conformation could potentially increase binding affinity by reducing entropy factors,^{18–21} we designed analogues of pTyr in which various torsion angles were constrained to those exhibited by the p56^{lck} SH2 domain-bound pTyr. The ability of these monomeric units to compete with larger pTyr-containing peptides for binding to SH2 domain fusion proteins is reported in this study.

Design of Conformationally Constrained pTyr Analogues

The X-ray coordinates of the pTyr residue from the previously reported structure of the high-affinity phosphopeptide E-P-Q-pY-E-E-I-P-I-Y-L bound to the p56^{lck} SH2 domain^{10,22} provided the basis for defining target conformations of constrained pTyr mimetics (Figure 1). The *N*^α-acetyl-*O*-phospho-*L*-tyrosine amide analogue (1) was designed as a flexible monomeric pTyr mimetic in which the *N*^α-acetyl carbonyl oxygen served to retain the hydrogen-bonding interactions normally afforded by the glutamyl carbonyl in the parent peptide. Likewise, 1 was prepared in the carboxamide form to approximate the pTyr-peptide amide bond normally present in the peptide structure. Methanobenzazocine 2 contained a bicyclic ring structure which restrained χ_1 , χ_2 , and ϕ

Scheme 1



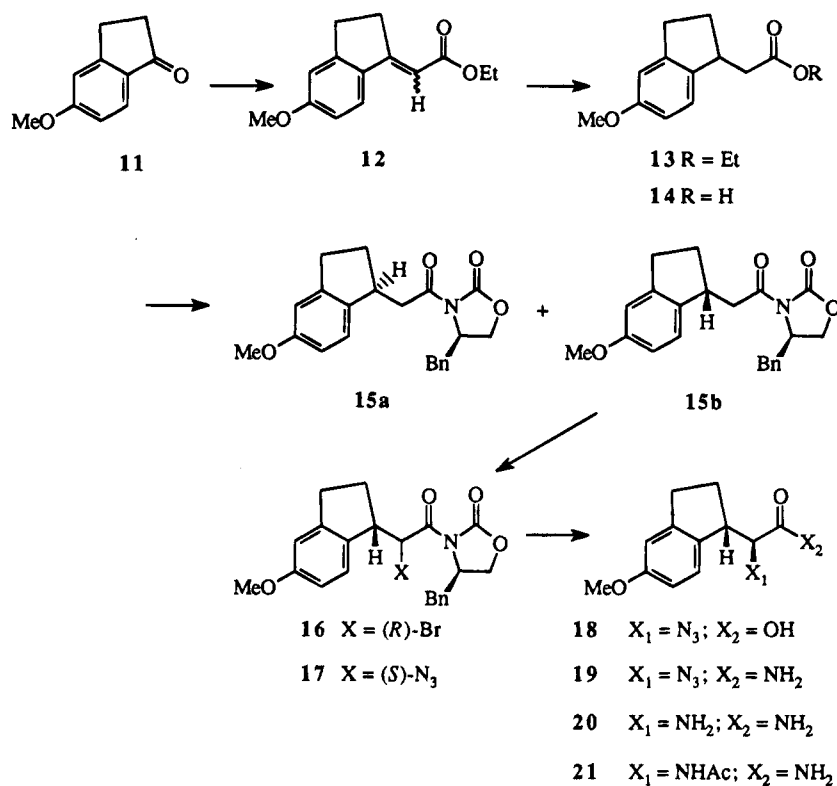
torsion angles to values closely approximating those found in the bound pTyr (Figure 1). Compound 2 had the disadvantage in that it lacked the tyrosyl carboxamide group of the parent tyrosyl residue. Alternatively, indanylglycine analogue 3 possessed the tyrosyl carboxamide group and restrained the χ_2 angle to near that found in the bound pTyr; however this analogue had conformationally unrestrained χ_1 and ϕ torsion angles (Figure 1). Indanylglycines have been used previously as conformationally constrained phenylalanyl analogues.^{23,24}

Synthesis

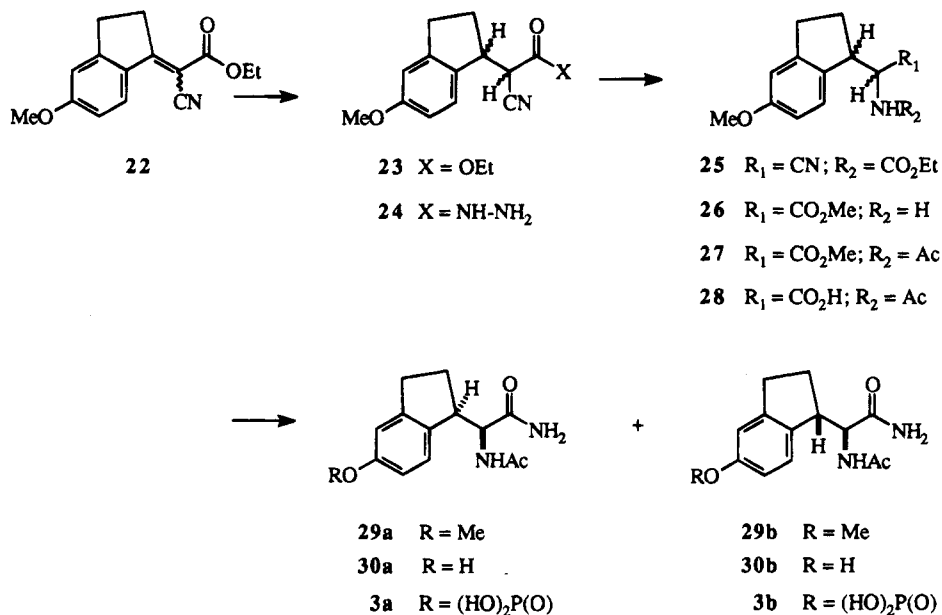
Preparation of *N*^α-acetyl-*O*-phosphoro-*L*-tyrosine amide (1) was achieved by phosphitylating commercially available *N*^α-acetyl-*L*-tyrosine amide with di-*tert*-butyl *N,N*-diisopropylphosphoramidite followed by oxidation (*m*-chloroperoxybenzoic acid) to the *tert*-butyl-protected phosphate and deprotection with 90% aqueous TFA. This approach was used to prepare all phosphate derivatives encompassed by this study.²⁵

Synthesis of phosphorylated methanobenzazocine 2 proceeded through the *N,O*-bis-methyl derivative 7 (Scheme 1). Preparation of 7 closely followed the previously reported route for the preparation of the 9-methoxy isomer.²⁶ This relies upon a key Mannich condensation/cyclization of 3,4-dihydro-6-methoxy-1-methyl-2(1*H*)-naphthalene-2-one (6) which was prepared in a manner similar to that of the 7-methoxy isomer.²⁷ Although desmethyl compound 5, which is the immediate precursor to 6, is commercially available, it proved more economical to derive it starting from the less expensive 2,6-dimethoxynaphthalene (4).²⁸ Compound 7 was *N*-demethylated to 8 using α -chloroethyl

Scheme 2



Scheme 3



chloroformate,²⁹ acetylated to **9**, and then *O*-demethylated³⁰ to give phenolic **10**. Phosphorylation provided the crude *tert*-butyl-protected phosphate, which upon treatment with aqueous 90% TFA and HPLC purification gave the desired final product (\pm)-**2**.

Enantioselective synthesis of 1'*R*,2*S*-**29a** was initially attempted using the chiral sultam method previously reported by Chassaing for the preparation of the corresponding constrained indanylglycine derivative which lacks the hydroxyl substituent at the 5'-position of the indane ring.^{24,31} Electronic differences imposed by oxygen substitution at the indane ring 5'-position of our compound prevented the successful application of this approach in our hands.

An alternative asymmetric synthesis was attempted using the Evans approach,³² which has also previously been used to prepare chiral indanylglycine derivatives.²³ As shown in Scheme 2, Wittig-Horner reaction of triethyl phosphonoacetate on commercially available 5-methoxyindan-1-one (**11**)³³ yielded ethyl ester **12** as an 87:13 mixture of *E/Z*-isomers. This was then hydrogenated to **13** and subjected to alkaline hydrolysis, yielding (\pm)-5'-methoxy-1'-indaneacetic acid (**14**). Resolution was accomplished by conversion into diastereomeric [3(1'*R*),4*R*]- and [3(1'*S*),4*R*]- (indanylacetyl)-oxazolidinones **15a,b** using commercially available (*R*)-(+)-4-(phenylmethyl)-2-oxazolidinone. Diastereomer **15b**, which bears the undesired *S*-configuration at the ben-

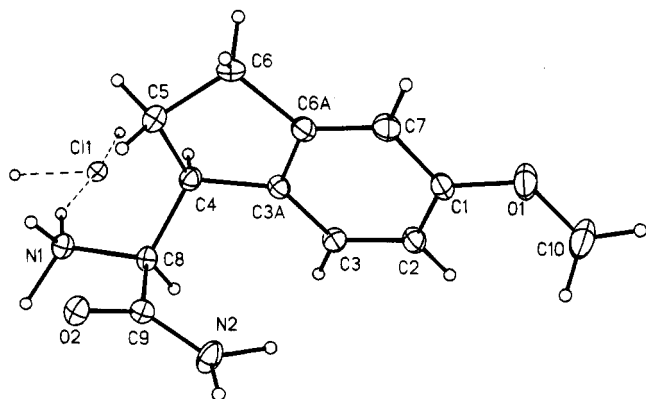


Figure 2. Thermal ellipsoid plot of **20**·HCl verifying a 1'*S*,2'*S*-configuration. Dashed lines are hydrogen bonds to the Cl ion. Only the hydrogen atoms are shown for symmetry-related molecules.

zylic 1''-position, was obtained by crystallization of the mixture. The *S*-absolute configuration was determined by X-ray crystallography at a subsequent stage (compound **20**). Diastereomer **15a** having the desired benzylic 1''*R*-configuration was obtained as a resin after tedious chromatography. Using the undesired 1''*S*-diastereomer **15b**, the *S*- α -amino group was introduced according to the method of Evans.³² This required a multistep process involving the initial addition of an *R*-bromine (compound **16**), S_N2 displacement by azide to give the 2*S*-configuration (compound **17**), and finally hydrogenolytic reduction of the azide, providing amine **20** after removal of the oxazolidinone chiral auxiliary. Several unsuccessful attempts were made to convert the desired 1''*R*-diastereomer **15a** to enantiomerically pure (1'*R*,2'*S*)-*N*^α-acetyl-2-(5'-methoxy-1'-indanyl)glycine amide (**29a**). It was therefore necessary to utilize an alternate racemic approach.

Preparation of the racemic indanylglycine amides **29a,b** followed the general procedure of Gagnon et al.³⁴ for the synthesis of amino acids from unsubstituted cyanoacetic esters (Scheme 3). The starting ethyl α -cyano-1-indaneacetate **23**, which was obtained as a racemic mixture of diastereomers following NaBH₄ reduction of **22**,³⁵ was converted via a Curtis rearrangement to an inseparable mixture of diastereomeric (\pm)-methyl 2-(5'-methoxy-1'-indanyl)glycinates **26**. Separation of *N*-acetylated diastereomeric amides **29a,b** was subsequently achieved chromatographically. Assignment of relative stereochemistries was based upon X-ray analysis of **29a** and by comparison of the NMR spectrum of **29b** with that of compound **21**, which was obtained by enantioselective synthesis. Demethylation of **29** using BBr₃ required treatment with a strong cation exchange resin to break boron complexes. Finally, phosphorylation of the resulting phenols **30a,b** was achieved as previously described to yield products **3a,b** as racemates.

Results and Discussion

X-ray Crystallography. The molecular structure of **20**·HCl revealed its absolute configuration to be 1'*S*,2'*S* (Figure 2). This indicated that the Evans *R*(+)-chiral auxiliary directed introduction of the amino functionality at the α -carbon in the desired *S*-configuration, consistent with previous reports.³² Unfortunately, the stereochemistry at the indanyl benzylic carbon was *S* rather

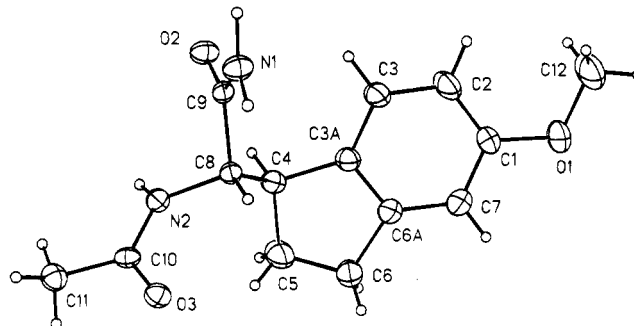


Figure 3. Thermal ellipsoid plot of **29a** showing a relative 1*R*,2*S*-configuration.

than *R*, as required for the proper χ_1 angle. This necessitated preparation of diastereomeric indanylglycines (\pm)-**29a,b** in a nonstereoselective manner. Compound (\pm)-**29b** exhibited TLC and NMR identical to that obtained on compound **21**. Since compound **21** was derived directly from **20** by acetylation, compound **29b** possessed the same relative 1'*S*,2'*R*-configuration found in **20**. The relative 1'*R*,2'*S*-configuration which was assigned to compound (\pm)-**29a** based on this analysis was subsequently confirmed by X-ray crystallography performed on **29a** (Figure 3). The final phosphorylated indanylglycine (\pm)-**3a**, which was derived from **29a**, therefore possessed the relative stereochemistries consistent with the p56^{lck} SH2 domain-bound pTyr residue, as shown in Figure 1.

NMR Spectroscopy. Proton assignments for compounds **2**, **9**, **10**, and **15–17** were facilitated by 2D COSY, long range COSY (LRCOSY),³⁶ and HETCOR experiments at 250 and 500 MHz. Intermediates *en route* to the indanylglycine derivatives **30** were assigned by COSY data. Spectra for compounds incorporating the Evans' chiral auxiliary (**15–17**) were generally first order, but the coupling constant data for the H2–H1' protons were not diagnostic for a particular diastereomer, i.e., the intermediate values of the couplings (4.5–7 Hz) were indicative of conformational averaging on the NMR time scale. On the other hand, data for the methanobenzazocine compounds **2**, **9**, and **10** were more informative. The ¹H NMR spectrum of **9** revealed a mixture of two distinct isomeric forms. These were attributed to two slowly interconverting rotomers (ca. 3:1) about the *N*-acetyl amide bond. The relatively inflexible tricyclic systems revealed an extensive array of long range couplings between protons at carbons C2–C6 and C11. The locked chair form of the bridged pyrrolidine ring situates the equatorial protons in a series of "W" relationships allowing several 4-bond coupling interactions. This was evident in the fine structure of the multiplets in the 1D spectra and was corroborated by the enhancement of long range cross-peaks in the LRCOSY spectra (65 ms delay for evolution of long range couplings). A more striking feature of this spectrum was the large difference in chemical shift ($\Delta\delta$) for the respective methylene protons of C4 of the major isomer and C2 of the minor isomer. Signals for these protons were separated by nearly 2 ppm. Inspection of models shows that if the amide group is kept planar, the carbonyl oxygen completely eclipses the equatorial proton at either C2 (H2_{eq}-CO synclinal, minor isomer) or C4 (H4_{eq}-CO synclinal, major isomer) placing this hydrogen directly in the shielding cone of the carbonyl electron cloud. Thus, the higher field proton for each

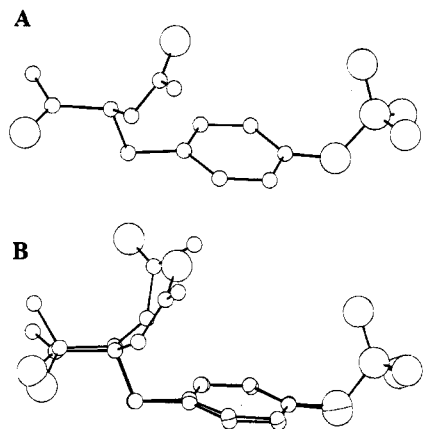


Figure 4. (A) p56^{lck} SH2 domain pTyr residue excised from the bound phosphopeptide E-P-Q-pY-E-E-I-P-I-Y-L. (B) Overlap of energy-minimized *N*-acetyl tyrosyl amide with the p56^{lck} SH2 domain-bound pTyr residue.

isomer is probably equatorial. Assignment of the major rotamer as H_{4eq}-CO synclinal was based on the large $\Delta\delta$ of the acetyl methyl signals. The acetyl methyl singlet for the major rotamer of compounds **2**, **9**, and **10** resonated between 1.35 and 1.40 ppm. This rotamer places the acetyl methyl group almost directly over the aromatic ring in the strongly shielding region of the aromatic π -cloud. The acetyl methyl signal for the minor isomer was found at the more typical chemical shift value of 1.8–2.0 ppm. This assignment was corroborated by molecular modeling studies (see below). Assuming that SH2 domain binding affinity is highly dependent on the appropriate amide torsion angle, there would be an intrinsic lowering of the biological activity of compound **2** since only the minor isomer aligns closely with the crystal structure of the bound pTyr.

Molecular Modeling Studies. The three-dimensional conformation of an SH2 domain-bound pTyr residue was derived from the X-ray structure of the peptide sequence E-P-Q-pY-E-E-I-P-I-Y-L complexed to a p56^{lck} SH2 domain fusion protein.¹⁰ The pTyr residue was excised and truncated at the C-terminal end as its primary amide and at its N-terminal end as its *N*^α-acetyl amide. The resulting monomeric *N*^α-acetyl-*O*-phosphoro-L-tyrosine amide exhibited χ_1 and χ_2 angles of 163.1° and -91.0°, respectively (Figure 4A). Independent conformational analysis of unbound *N*^α-acetyl-L-tyrosine amide using molecular mechanics (CHARMM³⁷) was performed by rotating χ_1 , χ_2 , and ϕ torsion angles. The torsional energies of χ_1 , as calculated by AM1 semiempirical quantum mechanics (MOPAC 6.0³⁸) from 0° to 360° in 10° increments, indicated three χ_1 energy minima at angles of 180°, -90°, and 81° separated by less than 0.3 kcal/mol. After refinement using *ab initio* methods (with 6-31G** basis set, GUASSIAN 92³⁹), a resulting energy-minimized structure ($\chi_1 = 179.7^\circ$) was shown to exhibit a high degree of congruence with the bound pTyr residue (Figure 4B). Conformational differences between the bound pTyr structure and energy-minimized *N*^α-acetyl-L-tyrosine amide arise mainly from torsional distortions of the *N*^α-acetyl-L-tyrosine amide which arise by intramolecular hydrogen bonds in the isolated molecule. The importance of these hydrogen bonds would be significantly diminished in solution.

In a similar manner, methanobenzazocine **10** was examined for its ability to overlap the bound pTyr

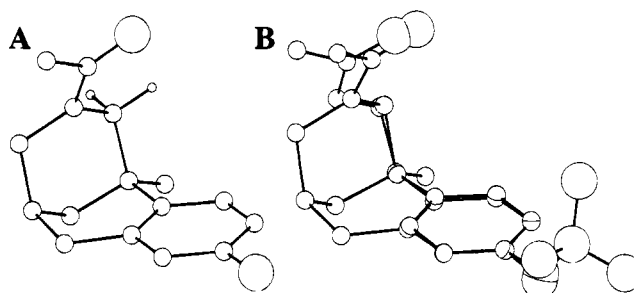


Figure 5. (A) Energy-minimized structure of compound **10** showing the major *N*-acetyl rotamer. (B) Overlap of panel A with the p56^{lck} SH2 domain-bound pTyr residue.

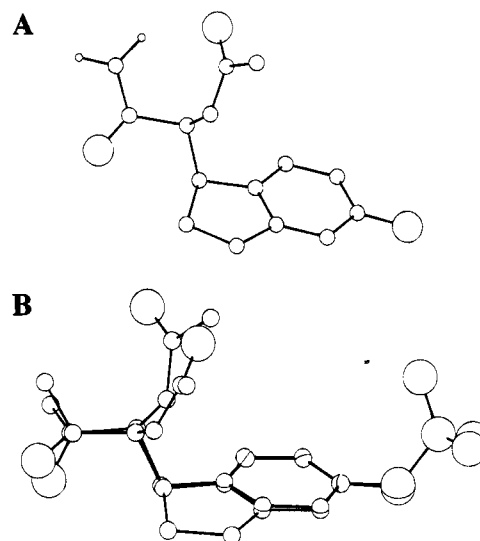


Figure 6. (A) Energy-minimized structure of compound **30a**. (B) Overlap of panel A with the p56^{lck} SH2 domain-bound pTyr residue.

structure. The rigid tricyclic ring system maintained fixed χ_1 and χ_2 angles of 177.8° and -87.1°, respectively, with conformational variability residing primarily in 180° rotational isomerism about the *N*-acetyl amide bond (Figure 5A). Energy differences between these two amide conformations were 0.93, 0.78, and 1.75 kcal/mol as determined by molecular mechanics, PM3 semiempirical quantum mechanics, and *ab initio* (6-31G) methods respectively, indicating that either rotamer is energetically permissible. One of these rotamers (H_{2eq}-CO synclinal) results in proper alignment for overlap of the *N*^α-acetamide functionality with the *N*-proximal glutamyl carboxyl of the bound pTyr residue, as shown in Figure 5B. NMR studies (see above) indicated that this rotamer is present in an approximate 1:3 ratio relative to the more abundant H_{4eq}-CO synclinal conformer in solution (DMSO).

Indanylglycine compound **30a** was likewise subject to a conformational analysis using molecular mechanics on the χ_1 and ϕ torsion angles, AM1 on the χ_1 torsion angle, and *ab initio* (6-31G) on the low-energy conformation suggested by AM1. The resulting minimized structure provided a remarkably close coincidence with the bound pTyr pharmacophore (Figure 6B). Diastereomeric indanylglycine **30b** was likewise subjected to conformational analysis using molecular mechanics and AM1 calculations. The low-energy conformation shown in Figure 7A (AM1 energy = -109.7 kcal/mol) is only slightly higher than the global energy minimum (-111.4 kcal/mol; AM1). As with diastereomer **30a**, this con-

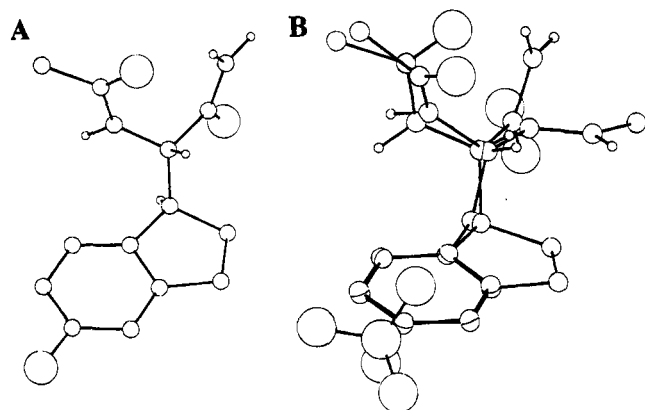


Figure 7. (A) Energy-minimized structure of compound **30b**. (B) Overlap of panel A with the p56^{lck} SH2 domain-bound pTyr residue.

formation aligns well with the Lck-bound pTyr (Figure 7B). Docking of methanobenzazocine **10** or indanylglycines **30a,b** into the p56^{lck} SH2 domain by overlaying on the bound pTyr residue did not result in any apparent significant adverse steric interactions.

SH2 Domain Binding. *In vitro* SH2 domain binding assays measured the ability of monomeric pTyr analogues to compete with larger high-affinity radiolabeled pTyr peptides in each of six different SH2 domains: Lck, Src, Grb2, and the C-terminal SH2 domains of PLC γ (PLC γ -C) and the p85 subunit of PI-3 kinase (p85-C), as well as the N-terminal SH2 domain of SH PTP2. The results of these studies (Table 1) indicate that inhibition constants of the monomeric pTyr analogues were either

above that measured or in the millimolar range. In spite of this, slight variations in potency among the analogues may indicate subtle differences in binding interactions which are worth considering. First, it can be observed that capping the amino and carboxyl termini of pTyr as the *N*-acetyl and carboxamide functionality respectively [(L)-**1**] resulted in a 2–3-fold increase in binding potency relative to free pTyr. This enhancement in binding is consistent with removal of potentially adverse interactions due to free pTyr's zwitterionic character and introduction of key hydrogen-bonding interactions afforded by the *N*-acetyl carbonyl and the carboxamido hydrogens. It can also be seen that the conformationally constrained indanylglycine derivatives (\pm)-**3a,b** did not exhibit increased binding potency. Part of the loss in potency of the indanylglycines relative to (L)-**1** may be attributable to the fact that these compounds were prepared in racemic form. More fundamental is the possibility that entropy gains achieved by conformational constraints may have been minimal. Since the peptidyl pTyr residue itself binds in a near global energy minimum conformation, it could be expected that a large population of free pTyr conformers would exist naturally in the correct, bound conformation without the aid of constraints. This could reduce advantages normally achieved by conformational restrictions. It should also be noted that the conformation of the bound pTyr residue may not reflect the conformation of the free ligand which is recognized during the initial SH2 domain binding process, since it is known that upon ligand binding SH2 domains undergo conformational changes.^{11,40} If the pTyr residue

Table 1. Inhibition Constants of pTyr Analogues against Various SH2 Domain Constructs

compound	ID ₅₀ \pm SD (mM)					
	Lck	Src	PLC γ -C	p85-C	Grb2	SH PTP2-N
 (L)-pTyr	≈ 5	3.5 ± 0.4	2.3 ± 0.9	3.5 ± 0.2	6.2 ± 3.7	>33
 (L)- 1	>3	1.0 ± 0.7	0.4 ± 0.17	1.5 ± 0.2	N.D.	>3
 (\pm)- 2	>3	0.9 ± 0.1	>3	1.3 ± 0.8	N.D.	>3
 (\pm)- 10	>6	>6	>6	>5	N.D.	>3
 (\pm)- 3a	>3	>3	>3	≈ 1.5	>3	>3
 (\pm)- 3b	≈ 1.5	>3	>3	≈ 1.5	>3	>3

itself is also subjected to conformational distortion during the binding process, constraining the pTyr residue to the final bound conformation may actually reduce affinity.

Of note also are the results obtained with methanobenzazocine analogue (\pm)-**2**. While not having measurable affinity against the Lck SH2 domain for which it was designed, it did maintain potency equivalent to *N* $^{\alpha}$ -acetyl pTyr amide [(L)-**1**] against the Src and p85-C SH2 domains. This is particularly noteworthy since racemic (\pm)-**2** contains only 50% of what would be expected to be the active enantiomer and it lacks appropriate hydrogen-bonding functionality normally afforded by the pTyr's carboxamide group. Additionally, it has approximately 75% of its *N*-acetyl rotamers (as determined in solution) situated opposite to the geometry need for alignment with the bound pTyr. In the unconstrained *N* $^{\alpha}$ -acetyl pTyr amide [(L)-**1**], rotation through ϕ can reverse improper acetamido cis/trans geometry, while this is not possible for **2**, where the effective ϕ angle is fixed. Since potency equivalent to *N* $^{\alpha}$ -acetyl pTyr amide was achieved despite these drawbacks, modification of **2** could provide a starting point for the development of more potent, small molecule SH2 domain inhibitors. However, current results suggest that high-affinity SH2 domain binding requires interactions extending beyond the pTyr binding pocket.

Experimental Section

Synthesis. Petroleum ether was of the boiling range 35–60 °C, and removal of solvents was performed by rotary evaporation under reduced pressure. Silica gel filtration was carried out using TLC grade silica gel (5–25 μ m; Aldrich). Preparative HPLC was conducted using a Vydac preparative C₁₈ peptide and protein column with a flow rate of 10 mL/min. Melting points were determined on a Mel Temp II melting point apparatus and are uncorrected. Elemental analyses were obtained from Atlantic Microlab Inc., Norcross, GA, and are within 0.4% of theoretical values unless otherwise indicated. Fast atom bombardment mass spectra (FABMS) were acquired with a VG Analytical 7070E mass spectrometer under the control of a VG 2035 data system. ¹H NMR data were obtained on Bruker AC250 (250 MHz) or, if indicated, AMX500 (500 MHz) instruments and are reported in ppm relative to TMS and referenced to the solvent in which they were run. COSY spectra were run at 500 MHz in magnitude mode. The delay for long range coupling in the LRCOSY was set to 65 ms.

***N* $^{\alpha}$ -Acetyl-O-phosphoro-L-tyrosine Amide (**1**).** To a suspension of *N* $^{\alpha}$ -acetyl-L-tyrosine amide (111 mg, 0.50 mmol) and 1*H*-tetrazole (114 mg, 1.50 mmol) in anhydrous DMF (1 mL) was added di-*tert*-butyl *N,N*-diisopropylphosphoramidite (Novabiochem; 173 μ L, 0.62 mmol), and the reaction mixture was stirred at room temperature (1 h). After the mixture was cooled to –78 °C, 85% *m*-chloroperoxybenzoic acid (119 mg, 0.65 mmol) in anhydrous CH₂Cl₂ (2 mL) was added and allowed to react at 0 °C for 30 min. The mixture was diluted with chilled CHCl₃ (100 mL), washed with ice-cold portions of 0.05 N HCl (2 \times 50 mL) followed by aqueous NaHCO₃ (2 \times 50 mL), dried (Na₂SO₄), and then taken to dryness under high vacuum. The crude material was purified by reverse phase HPLC [linear gradient from 0% B to 10% B over 30 min; solvent A = 0.05% aqueous TFA; solvent B = 0.05% TFA in acetonitrile; product elution time, 8.4 min (*k'* = 0.6)] to yield 112 mg (74%) of **1** as a white solid contaminated with diisopropylamine. Repurification provided **1** as an amorphous white solid (35 mg): ¹H NMR (DMSO-*d*₆) δ 8.00 (d, *J* = 8.4 Hz, exchangeable 1H, –NHAc), 7.43 (s, exchangeable 1H, NH₂), 7.03 (AB quartet, 4H, *o,m*-aromatic H), 7.01 (br s, exchangeable 1H, NH₂), 4.36 (m, 1H, H-2), 2.89 (dd, *J* = 4.7 and 13.8 Hz, 1H, H-3), 2.66 (dd, *J* = 9.5 and 13.8 Hz, 1H, H-3'),

1.78 (s, 3H, CH₃CO); FABMS (Gly; –ve) *m/z* 301 (M – H)[–]. Anal. (C₁₁H₁₅N₂O₆· $\frac{1}{2}$ H₂O), C, H, N.

(\pm)-**1,3-Dimethyl-1,2,3,4,5,6-hexahydro-1,5-methano-8-methoxy-1-methyl-3-benzazocine (**7**).** A mixture of 3.0 g (16 mmol) of **6** (prepared in a manner similar to the 7-methoxy isomer²⁷), methylamine hydrochloride (1.38 g, 20 mmol), and 36% aqueous formaldehyde (5.3 mL, 63 mmol) in acetic acid (30 mL) was stirred at reflux (5 h). Solvent was reduced in volume by distillation, and the residue was partitioned between 2 N HCl (75 mL)/CHCl₃ (3 \times 25 mL). The aqueous layer was made alkaline (KOH), extracted with CHCl₃ (3 \times 50 mL), washed with brine (50 mL), dried (Na₂SO₄), and taken to dryness. The resulting dark syrup was passed down a silica pad using CHCl₃ to provide intermediate (\pm)-1,3-dimethyl-1,2,3,4,5,6-hexahydro-1,5-methano-8-methoxy-1-methyl-3-benzazocin-11-one as 1.65 g of a yellow syrup. This was mixed with hydrazine hydrate (2.61 mL, 54 mmol) and 2.57 g (40 mmol) of 88% KOH and stirred at 190 °C in 20 mL of diethylene glycol (5 h). The reaction mixture was cooled to room temperature and partitioned between H₂O (150 mL) and ether (4 \times 50 mL), and then the combined ether layers were washed with brine (100 mL), dried (Na₂SO₄), and taken to dryness. Purification by silica gel chromatography (CHCl₃ and then CHCl₃:ethyl acetate (1:1)) provided **7** as cream-colored crystals, 533 mg (14% overall yield): mp 43–45 °C; ¹H NMR (CDCl₃) δ 7.07 (d, *J* = 8.5 Hz, 1H, H-10), 6.53–6.63 (m, 2H, H-7, H-9), 3.68 (s, 3H, –OCH₃), 3.03 (dd, *J* = 7.2 and 17.5 Hz, 1H, H-4), 2.80 (m, 1H, H-2), 2.78 (br d, *J* = 17.5 Hz, 1H, H-4'), 2.43 (br d, *J* = 10.4 Hz, 1H, H-6), 2.13 (m, 1H, H-5), 2.05 (m, 1H, H-2'), 2.03 (s, 3H, –NCH₃), 1.76 (d, *J* = 10.4 Hz, 1H, H-6'), 1.66 (dq, *J* = 12.3 and 2.3 Hz, 1H, H-11), 1.35 (br dd, *J* = 12.3 and 2.2 Hz, 1H, H-11'), 1.21 (s, 3H, CH₃); FABMS (NBA; +ve) *m/z* 232 (M + H)⁺.

(\pm)-**3-Acetyl-1,2,3,4,5,6-hexahydro-1,5-methano-8-methoxy-1-methyl-3-benzazocine (**9**).** To **7** (392 mg, 1.70 mmol) in anhydrous CH₂Cl₂ (5 mL) at 0 °C was added α -chloroethyl chloroformate (276 μ L, 254 mmol), and the yellow solution was stirred initially at 0 °C (10 min) and then at reflux (6 h). The solvent was removed and the residue refluxed (2 h) in anhydrous MeOH (10 mL), and then the solvent was removed to yield crude secondary amine **8**·HCl. This was stirred at room temperature (2 h) with acetic anhydride (240 μ L, 2.6 mmol) and *N*-methylmorpholine (466 μ L, 4.2 mmol) in anhydrous DMF (1 mL) and then subjected to an extractive workup (0.2 N HCl in brine/CHCl₃), dried (Na₂SO₄), and evaporated to an oil. The oil was dissolved in a small volume of ether: petroleum ether and cooled to –78 °C, and the supernatant was decanted. The resulting gum was crystallized from ether: petroleum ether to yield light tan crystals (236 mg) which were combined with a reworkup of the filtrate to provide **9** as light tan crystals (326 mg, 74%): mp 101–102 °C; ¹H NMR (major rotamer) (CDCl₃) δ 7.18 (d, *J* = 8.6 Hz, 1H, H-10), 6.68 (dd, *J* = 8.6 and 2.4 Hz, 1H, H-9), 6.60 (d, *J* = 2.4 Hz, 1H, H-7), 4.79 (m, 1H, H-4), 3.76 (s, 3H, CH₃O-), 3.32 (m, 1H, H-2), 3.03 (m, 2H, H-2' and H-6), 2.85 (d, *J* = 17.7 Hz, 1H, H-6'), 2.70 (br m, 1H, H-4'), 2.22 (m, 1H, H-5), 1.86 (br m, 1H, H-11), 1.65 (br m, 1H, H-11'), 1.39 (s, 3H, CH₃CO-), 1.37 (s, 3H, CH₃); FABMS (NBA; +ve) *m/z* 260 (M + H)⁺. Anal. (C₁₆H₂₁NO₂) C, H, N.

(\pm)-**3-Acetyl-1,2,3,4,5,6-hexahydro-8-hydroxy-1,5-methano-1-methyl-3-benzazocine (**10**).** To a solution of **9** (206 mg, 0.80 mmol) in anhydrous CH₂Cl₂ (5 mL) at –78 °C was added BBr₃, 1.0 M in CH₂Cl₂ (800 μ L), and the mixture was stirred at 0 °C (2.5 h). An additional equivalent of BBr₃ was added, and the reaction was allowed to continue at 0 °C (1 h), and then quenched by addition of anhydrous MeOH (2 mL). The product was taken to dryness and re-evaporated from anhydrous MeOH (2 mL). The resulting residue was partitioned between NaHCO₃ in brine/CHCl₃ and dried (Na₂SO₄), and the solvent was removed to yield crude **10** quantitatively as a cream-colored solid (205 mg). An analytical sample was prepared by suspending in MeOH and filtering, providing white crystals: mp 217–220 °C; ¹H NMR (major rotamer) (DMSO-*d*₆) δ 9.07 (s, 1H, phenolic OH), 7.13 (d, *J* = 8.4 Hz, 1H, H-10), 6.51 (dd, *J* = 2.5 and 8.4 Hz, 1H, H-9), 6.39 (br d, *J* = 2.5 Hz, 1H, H-7), 4.55 (br d, *J* = 12.7 Hz, 1H, H-4), 3.32 (m, 1H, H-2), 2.99 (d, *J* = 12.9 Hz, 1H, H-2'), 2.92 (dd, *J* = 6.6

and 17.8 Hz, 1H, H-6), 2.63 (dist d, 1H, H-4'), 2.56 (m, 1H, H-6'), 2.11 (m, 1H, H-5), 1.72 (m, 2H, H-14, H-11'), 1.30 (s, 3H, CH₃CO), 1.19 (s, 3H, CH₃); FABMS (NBA; +ve) *m/z* 246 (M + H)⁺. Anal. (C₁₅H₁₉NO₂·¹/₄H₂O) C, H, N.

(±)-**3-Acetyl-1,2,3,4,5,6-hexahydro-1,5-methano-1-methyl-8-(O-phosphoro)-3-benzocaine (2)**. A suspension of **10** (61 mg, 0.25 mmol) and 1*H*-tetrazole (57 mg, 0.75 mmol) in anhydrous DMF (1 mL) was briefly warmed to effect a solution and then stirred at room temperature. To this was added di-*tert*-butyl *N,N*-diisopropylphosphoramidite (87 μL, 0.31 mmol), and the solution was stirred at room temperature (3 h). The reaction mixture was then cooled to -78 °C, a solution of 85% *m*-chloroperoxybenzoic acid (66 mg, 0.32 mmol) in anhydrous CH₂Cl₂ (1 mL) was added, and the reaction continued at 0 °C (40 min). The mixture was diluted with chilled CHCl₃ (100 mL), washed with ice-cold portions of 0.05 N HCl (2 × 50 mL) and aqueous NaHCO₃, and then dried (Na₂SO₄) and taken to dryness to yield the crude *tert*-butyl-protected intermediate. This was stirred at room temperature with 90% aqueous TFA (1 h) and then taken to dryness under high vacuum. The resulting syrup was crystallized from acetonitrile to provide phosphate **2** as white crystals (64 mg, 79%): mp 226–228 °C; ¹H NMR (major rotamer) (DMSO-*d*₆) δ 7.33 (d, *J* = 8.6 Hz, 1H, H-10), 6.91 (dd, *J* = 1.9 and 8.6 Hz, 1H, H-9), 6.82 (br d, *J* = 1.9 Hz, 1H, H-7), 4.56 (br d, *J* = 13.0 Hz, 1H, H-4), 3.39 (br d, *J* = 13.1 Hz, 1H, H-2), 3.02 (d, *J* = 13.1 Hz, 1H, H-2'), 2.97 (dd, *J* = 17.6 and 6.5 Hz, 1H, H-6), 2.67 (d, *J* = 2.0 and 12.3 Hz, 1H, H-4'), 2.63 (d, *J* = 17.8 Hz, 1H, H-6'), 2.16 (m, 1H, H-5), 1.75 (m, 1H, H-11, H-11'); FABMS (Gly; -ve) *m/z* 324 (M - H)⁻. Anal. (C₁₅H₂₀NO₅P) C, H, N.

Ethyl 2-(5'-Methoxyindan-1'-ylidene)acetate (12). Triethyl phosphonoacetate (10.0 mL, 50 mmol) was added rapidly dropwise to a stirred suspension of 80% NaH in oil (1.50 g, 50 mmol) in anhydrous THF (50 mL), and the reaction mixture was stirred at room temperature (1 h). A solution of 5-methoxyindan-1-one (6.75 g, 42 mmol) in anhydrous THF (50 mL) was added, and the resulting black mixture was stirred at reflux overnight. The solvent was removed, and the residual syrup was filtered through a silica pad using CHCl₃:petroleum ether (1:1) and then distilled under high vacuum. A white crystalline forerun was followed by a yellow oil, which was collected as product (3.78 g). The initial forerun was repurified by silica gel chromatography [CHCl₃:petroleum ether (1:2)] to provide additional product giving a combined yield of 6.11 g (63%). Crystallization occurred upon setting, with recrystallization from petroleum ether yielding light yellow crystals: mp 51–53 °C (lit.⁴¹ mp 52–54 °C); ¹H NMR (CDCl₃) δ 7.43 (d, *J* = 8.3 Hz, 1H, H-7'), 6.75 (br s, 1H, H-4'), 6.73 (dd, *J* = 8.3 and 2.2 Hz, 1H, H-6'), 6.08 (t, *J* = 2.4 Hz, 1H, H-2), 4.13 (q, *J* = 7.1 Hz, 2H, -OCH₂CH₃), 3.75 (s, 3H, OCH₃), 3.23 (m, 2H, H-2', H-2''), 2.96 (m, 2H, H-3', H-3''), 1.25 (t, 3H, -OCH₂CH₃).

(±)-**Ethyl 5'-Methoxy-1'-indaneacetate (13)**. A solution of **12** (11.55 g, 50 mmol) in EtOH (50 mL) was hydrogenated over 10% Pd-C (200 mg) under 40 psi H₂ (3 h with replenishing of H₂). Filtration through Celite and removal of solvent provided **13** as a colorless oil (11.3 g, 97%): ¹H NMR (CDCl₃) δ 7.06 (d, *J* = 8.3 Hz, 1H, H-7'), 6.77 (br d, 1H, H-4'), 6.72 (dd, *J* = 8.3 and 2.4 Hz, 1H, H-6'), 4.17 (q, *J* = 7.2 Hz, 2H, -OCH₂CH₃), 3.78 (s, 3H, OCH₃), 3.52 (m, 1H, H-1'), 2.86 (m, 2H, H-3', H-3''), 2.72 (dd, *J* = 15.3 and 5.6 Hz, 1H, H-2), 2.41 (dd, *J* = 15.3 and 9.0 Hz, 1H, H-2'), 2.38 (m, 1H, H-2'), 1.76 (m, 1H, H-2''), 1.28 (t, 3H, -OCH₂CH₃); FABMS (NBA; +ve) *m/z* 235 (M + H)⁺.

(±)-**5'-Methoxy-1'-indaneacetic Acid (14)**. A total of 11.0 g (47 mmol) of **13** was stirred at reflux (1.5 h) with LiOH·H₂O (4.92 g, 118 mmol) in a mixture of EtOH (50 mL) and H₂O (50 mL). The solution was partitioned between 1 N HCl (200 mL) and EtOAc (3 × 75 mL), dried (MgSO₄), taken to dryness, and crystallized from petroleum ether, yielding **14** as cream-colored crystals (8.0 g, 83%): mp 81–82 °C; ¹H NMR (CDCl₃) δ 7.10 (d, *J* = 8.2 Hz, 1H, H-7'), 6.78 (br s, 1H, H-4'), 6.73 (dd, *J* = 8.2 and 2.4 Hz, 1H, H-6'), 3.77 (s, 3H, OCH₃), 3.54 (m, 1H, H-1'), 2.87 (m, 2H, H-3', H-3''), 2.79 (dd, *J* = 5.5 and 15.6 Hz, 1H, H-2), 2.47 (dd, *J* = 9.1 and 15.6 Hz, 1H, H-2'), 2.43 (m, 1H, H-2'), 1.78 (m, 1H, H-2''); FABMS (NBA; -ve) *m/z* 358 (M + H)⁺. Anal. (C₁₂H₁₄O₃) C, H.

[3(1''R),4R]-3-[2'-(5''-Methoxy-1''-indanyl)acetyl]-4-(phenylmethyl)-2-oxazolidinone and [3(1''S),4R]-3-[2'-(5''-Methoxy-1''-indanyl)acetyl]-4-(phenylmethyl)-2-oxazolidinone (15a,b). To a suspension of 80% NaH in oil (165 mg, 5.5 mmol) in anhydrous THF (5 mL) at 0 °C was added a solution of **14** (1.03 g, 5.00 mmol) in anhydrous THF, and the mixture was stirred at 0 °C (10 min). The temperature was lowered to -78 °C, and pivaloyl chloride (678 μL, 5.5 mmol) was added. The reaction mixture was then stirred at 0 °C (45 min) and cooled to -78 °C. In a separate flask a total of 3.4 mL (5.5 mmol) of 1.6 M *n*-butyllithium in hexane was added to a solution of (*R*)-(+)-4-(phenylmethyl)-2-oxazolidinone (974 mg, 5.5 mmol) in anhydrous THF (10 mL) at -78 °C and the reaction mixture was stirred at -78 °C (30 min). This was added via cannula to the indanyl reaction mixture, and the resulting mixture was stirred at 0 °C (1 h). The solvent was removed and the residue subjected to an extractive workup (brine/EtOAc), dried (Na₂SO₄), and taken to dryness (2.2 g crude syrup). Crystallization (ether) provided **15b** as white crystals (640 mg, 70%). Repeated chromatography (CHCl₃:petroleum ether, from 1:1 to 1:0) provided **15a** as a resin (670 mg, 73%): FABMS (NBA; +ve) *m/z* 366 (M + H)⁺. **15b**: mp 115–117 °C; ¹H NMR (CDCl₃) δ 7.14–7.33 (m, 5H, aromatic), 7.10 (d, *J* = 8.2 Hz, 1H, H-7'), 6.72 (br s, 1H, H-4'), 6.66 (dd, *J* = 2.5 and 8.4 Hz, 1H, H-6'), 4.65 (m, 1H, H-11'), 4.12 (m, 2H, H-10', H-10''), 3.71 (s, 3H, OCH₃), 3.58 (m, 1H, H-1'), 3.35 (dd, *J* = 5.0 and 16.9 Hz, 1H, H-2), 3.28 (dd, *J* = 3.0 and 14.1 Hz, 1H, H-12'), 2.92 (dd, *J* = 16.9 and 9.0 Hz, 1H, H-2'), 2.83 (m, 2H, H-3''), 2.72 (dd, *J* = 9.7 and 13.3 Hz, 1H, H-12'), 2.36 (m, 1H, H-2''), 1.75 (m, 1H, H-2''); FABMS (NBA; +ve) *m/z* 366 (M + H)⁺. Anal. (C₂₂H₂₃NO₄) C, H, N.

[3(1''S,2'R),4R]-3-[2'-Bromo-2'-(5''-methoxy-1''-indanyl)acetyl]-4-(phenylmethyl)-2-oxazolidinone (16). To a solution of **15b** (356 mg, 1.0 mmol) in anhydrous CH₂Cl₂ (2 mL) at -78 °C was added diisopropylethylamine (209 μL, 1.2 mmol) followed by di-*n*-butylboron triflate (1.0 M) in CH₂Cl₂ (1.05 mL). The reaction mixture was stirred initially at -78 °C (15 min) and then at 0 °C (1 h). The temperature was lowered to -78 °C, a suspension of *N*-bromosuccinimide (195 mg, 1.1 mmol) in anhydrous CH₂Cl₂ (1 mL) was added rapidly via cannula at -78 °C, and the resulting brown solution was stirred at -78 °C (1 h). The reaction mixture was subjected to an extractive workup (1 N HCl in brine/EtOAc), dried (Na₂SO₄), and taken to dryness. Residue was passed down a silica pad (CHCl₃:petroleum ether, 3:1) yielding 367 mg of **16** contaminated with starting **15**.

[3(1''S,2'S),4R]-3-[2'-Azido-2'-(5''-methoxy-1''-indanyl)acetyl]-4-(phenylmethyl)-2-oxazolidinone (17). To a solution of impure **16** (157 mg, 0.35 mmol theoretical maximum) in anhydrous CH₂Cl₂ (5 mL) was added tetramethylguanidinium azide⁴² (167 mg, 1.1 mmol), and the mixture was stirred at room temperature overnight. The reaction mixture was applied directly to a silica pad and eluted with CHCl₃, yielding **17** contaminated with **15** which was carried from the previous step (126 mg of crude product).

(1'S,2S)-α-Azido-5'-methoxy-1'-indaneacetic Acid (18). To crude **17** (126 mg, 0.31 mmol theoretical maximum) in THF (1.5 mL) at 0 °C was added dropwise 0.5 N LiOH (1.2 mL, 0.6 mmol), and the reaction mixture was stirred at 0 °C (30 min). The mixture was partitioned between 0.5 N HCl (10 mL)/EtOAc (3 × 10 mL), dried (Na₂SO₄), and then taken to dryness and passed down a silica pad (CHCl₃), yielding **18** as a syrup (52 mg) contaminated with a small amount of 4-(phenylmethyl)-2-oxazolidinone.

(1'S,2S)-2-Azido-2-(5'-methoxy-1'-indanyl)acetamide (19). To a solution of **18** (67 mg, approximately 0.27 mmol) in anhydrous THF (1 mL) at -78 °C was added triethylamine (45 μL, 0.32 mmol), and the mixture was stirred at 0 °C (50 min). The reaction mixture was cooled to -78 °C, 25% aqueous NH₄OH (54 μL, 0.8 mmol) was added, and the reaction continued at 0 °C (40 min). The mixture was diluted with H₂O (10 mL), extracted with EtOAc (3 × 10 mL), washed with aqueous NaHCO₃ (1 × 10 mL), and dried (Na₂SO₄) and the solvent removed. The resulting residue was passed down a silica pad (CHCl₃), yielding **19** as a colorless resin (21 mg): ¹H NMR (CDCl₃) δ 7.07 (d, *J* = 8.3 Hz, 1H, H-7'), 6.72 (br s,

1H, H-4'), 6.64 (dd, $J = 2.5$ and 8.3 Hz, 1H, H-6'), 6.12 and 6.02 (br s, 1H, NH), 4.01 (d, $J = 5.0$ Hz, 1H, H-2), 3.71 (s, 3H, OCH₃), 3.69 (m, 1H, H-1'), 2.97 (m, 1H, H-3'), 2.81 (m, 1H, H-3''), 2.34 (m, 1H, H-2'), 2.03 (m, 1H, H-2'').

(1*S*,2*S*)-2-(5'-Methoxy-1'-indanyl)glycine Amide (20). A solution of **19** (48 mg) contaminated with 4-(phenylmethyl)-2-oxazolidinone was hydrogenated in MeOH (20 mL) over 10% Pd-C under 40 psi H₂ (3 h). Catalyst and solvent were removed, and the resulting residue was triturated with EtOAc to provide **20** as a white solid (13 mg). The EtOAc supernatant was passed down a silica pad, and impurities were eluted with 10% MeOH in EtOAc. In this manner an additional 10 mg of product was obtained, yielding combined **20** as 23 mg of a white solid: ¹H NMR (CD₃OD) δ 7.23 (d, $J = 8.3$ Hz, 1H, H-7'), 6.83 (br s, 1H, H-4'), 6.77 (dd, $J = 2.4$ and 8.3 Hz, 1H, H-6'), 4.06 (d, $J = 4.6$ Hz, 1H, H-2), 3.75 (s, 3H, OCH₃), 3.67 (m, 1H, H-1'), 2.97 (m, 1H, H-3'), 2.86 (m, 1H, H-3''), 2.35 (m, 1H, H-2'), 2.16 (m, 1H, H-2''); FABMS (NBA; +ve) m/z 221 (M + H)⁺. The structure of **20**-HCl was elucidated by X-ray diffractometry as described below.

N^o-Acetyl-(1*S*,2*S*)-2-(5'-methoxy-1'-indanyl)glycine Amide (21). To a suspension of **20** (10 mg, 0.045 mmol) in CHCl₃ (1 mL) at 0 °C was added triethylamine (12 μ L, 0.09 mmol) followed by acetic anhydride (12 μ L, 0.13 mmol). The reaction mixture was stirred at 0 °C (1 h) and then partitioned [1 N HCl (10 mL)/EtOAc (3 \times 10 mL)], dried (Na₂SO₄), and taken to dryness, yielding **21** as a white solid (6 mg, 51%). TLC and ¹H NMR were identical to those obtained on compound **29b**.

(\pm)-Ethyl α -Cyano-5'-methoxy-1'-indaneacetate (23). As previously reported³⁵ to a suspension of ethyl 2-cyano-2-(5'-methoxyindan-1'-ylidene)acetate (**22**) (13 g, 50 mmol) in 110 mL of THF:EtOH (10:1) at 0 °C was added NaHB₄ (1.90 g, 50 mmol), and the mixture was stirred at 0 °C (6.5 h). The reaction mixture was subjected to an extractive workup (1 N HCl/CHCl₃), dried (MgSO₄), and taken to dryness. The crude product (12.7 g) was passed down a silica pad using petroleum ether:CHCl₃ (2:1) to provide pure **23** as a light yellow oil (10.2 g, 79%) (lit.³⁵ 88%).

(\pm)- α -Cyano-5'-methoxy-1'-indaneacetohydrazide (24). To a solution of **23** (1.30 g, 5.0 mmol) in EtOH (10 mL) was added hydrazine hydrate (70 μ L, 5.5 mmol), and the solution was stirred at room temperature (3 days). The resulting thick white mass was filtered, yielding 720 mg of white solid, which was combined with 58 mg of additional solid obtained by working up the filtrate (778 mg, 64%): mp 128–131 °C; ¹H NMR (DMSO-*d*₆) δ 9.46 (br s, 1H, NH), 7.30 (d, $J = 8.3$ Hz, 1H, H-7'), 6.85 (br s, 1H, H-4'), 6.76 (dd, $J = 2.5$ and 8.3 Hz, 1H, H-6'), 4.50 (br d, 2H, NH₂), 3.74 (s, 3H, OCH₃), 3.61 (obscure d, 1H, H-2), 3.58 (m, 1H, H-1'), 2.92 (m, 1H, H-3'), 2.78 (m, 1H, H-3''), 2.20 (m, 1H, H-2'), 1.82 (m, 1H, H-2''); FABMS (NBA; +ve) m/z 246 (M + H)⁺. Anal. (C₁₃H₁₅N₃O₂) C, H, N.

(\pm)-1-[1'-(*N*-Carbomethoxyamino)-1'-cyanomethyl]-5-methoxyindane (25). To a thick suspension of **24** (4.36 g, 17.8 mmol) in a mixture of 37% HCl (10 mL), H₂O (15 mL), and ether (35 mL) at 0 °C was added a solution of NaNO₂ (1.47 g, 21.4 mmol) in H₂O. The solid rapidly dissolved, and the resulting biphasic mixture was stirred at 0 °C (1.5 h). The mixture was added to a separatory funnel, and the ether layer was collected, combined with ether extracts of the aqueous phase (2 \times 15 mL), washed with 1 N HCl (1 \times 25 mL), and dried (MgSO₄). The extract was diluted with absolute EtOH (50 mL) and the ether removed by rotary evaporation. Then, additional absolute EtOH was added (50 mL) and the yellow solution stirred at reflux (1 h). Removal of solvent provided crude (\pm)-**25** as a light orange oil sufficiently pure for further use (4.47 g, 92%): FABMS (NBA; +ve) m/z 275 (M + H)⁺.

(\pm)-Methyl 2-(5'-Methoxy-1'-indanyl)glycinate (26). A solution of **25** (4.0 g, 15 mmol) in a mixture of 88% formic acid (50 mL), 37% HCl (50 mL), and H₂O (50 mL) was stirred at reflux overnight, and the solvent was removed by rotary evaporation. The residue was taken to dryness repeatedly from anhydrous MeOH (4 \times 150 mL) and then stirred at reflux overnight with methanolic HCl (150 mL). Solvent was removed, residue was subjected to an extractive workup (NaH-

CO₃ in brine/CHCl₃) and dried (MgSO₄), and solvent was removed, yielding a brown syrup (2.83 g). Filtration through a silica pad (CHCl₃) provided product **26** sufficiently pure for further use (1.96 g, 56%). A sample was converted to the HCl salt and crystallized (ether:MeOH), yielding **26**-HCl as light yellow crystals: mp 150–152 °C; ¹H NMR (1:1 mixture of diastereomers A + B in DMSO-*d*₆) δ 7.17 (center of 2 d, H-7', A + B), 6.79 (center of 2 br s and 2 dd, H-4' and H-6', A + B), 4.40 and 4.35 (2 d, $J = 4.2$ and 5.7 Hz, H-2, A + B), 3.73 (s, 6H, 2 OCH₃, A + B), 3.71 (s, 3H, OCH₃, A), 3.64 (m, 2H, H-1', A + B), 3.60 (s, 3H, OCH₃, B), 2.70–3.0 (m, 4H, H-3' and H-3'', A + B), 1.8–2.5 (4 m, H-2', H-2'', A + B); FABMS (NBA; +ve) m/z 236 (M + H)⁺. Anal. (C₁₃H₁₇NO₃·HCl), C, H, N.

(\pm)-Methyl N^o-Acetyl-2-(5'-methoxy-1'-indanyl)glycinate (27). To a solution of **26** (1.93 g, 8.2 mmol) in CHCl₃ (50 mL) at 0 °C was added triethylamine (2.28 mL, 16 mmol) dropwise followed by acetic anhydride (850 μ L, 9.0 mmol). The reaction mixture was stirred at 0 °C (3 h) and then diluted with CHCl₃ (50 mL), washed with 1 N HCl (2 \times 50 mL), dried (MgSO₄), and taken to dryness, yielding **27** as a syrup in sufficient purity for further use (2.14 g, 96%): ¹H NMR (1:1 mixture of diastereomers A + B in DMSO-*d*₆) δ 7.08 (d, $J = 8.3$ Hz, 1H, H-7', A), 6.93 (d, $J = 8.3$ Hz, 1H, H-7', B), 6.77 and 6.74 (2 br s, 1H each, H-4', A + B), 6.72 and 6.69 (2 d, $J = 2.3$ and 2.0 Hz, 1H each, H-6', A + B), 5.88 (br d, $J = 8.3$ Hz, 1H, NH, A), 5.63 (br d, $J = 9.0$ Hz, 1H, NH, B), 4.98 (center of 2 dd, $J = 5.3$, 8.4 and 3.5 , 9.2 Hz, H-2, A + B), 3.78 (s, 3H, OCH₃, A), 3.77 (s, 6H, OCH₃, A + B), 3.71 (s, 3H, OCH₃, B), 3.75 and 3.62 (m, 1H each, H-1', A + B), 2.85 (center of 4 m, H-3', H-3'', A + B), 1.83–2.41 (4 m, H-2', H-2'', A + B), 1.95 and 1.93 (2 s, 3H each, CH₃CON⁻); FABMS (NBA; +ve) m/z 278 (M + H)⁺.

(\pm)-N^o-Acetyl-2-(5'-hydroxy-1'-indanyl)glycine (28). To a solution of **27** (1.93 g, 8.2 mmol) in MeOH (20 mL) was added 0.5 N LiOH (6 mL, 3.0 mmol), and the reaction mixture was stirred at room temperature. After 1.5 h an additional 6 mL (3.0 mmol) of 0.5 N LiOH was added and the reaction continued (2 h), and then MeOH was removed by rotary evaporation. The resulting solution was acidified with 1 N HCl (20 mL), extracted with CHCl₃ (3 \times 30 mL), dried (MgSO₄), and evaporated to yield **28** as a white foam (698 mg, 88%).

(\pm)-rel-(1*R*,2*S*)-N^o-Acetyl-2-(5'-methoxy-1'-indanyl)glycine Amide (29a) and (\pm)-rel-(1*S*,2*S*)-N^o-Acetyl-2-(5'-methoxy-1'-indanyl)glycine Amide (29b). To **28** (698 mg, 2.65 mmol) in anhydrous THF (25 mL) at –78 °C were added triethylamine (443 μ L, 3.18 mmol), and then pivaloyl chloride (392 μ L, 3.18 mmol), and the reaction mixture was stirred at 0 °C (30 min). The reaction mixture was cooled to –78 °C, and then 540 μ L (3 equiv) of 25% aqueous NH₄OH was added and the mixture was stirred at 0 °C (2 h). The suspension was partitioned between H₂O (50 mL) and CHCl₃ (3 \times 50 mL) and dried (MgSO₄) and solvent removed to yield crude product as a white solid (510 mg). Chromatographic purification [CHCl₃:MeOH:NH₄OH (98:2:1)] eluted first pivaloyl amide followed by **29a** (160 mg) and then **29b** (111 mg). (\pm)-**29a**: mp 253–258 °C; ¹H NMR (DMSO-*d*₆, 1 drop of DCl) δ 7.02 (d, $J = 8.2$ Hz, 1H, H-7'), 6.75 (br s, 1H, H-4'), 6.66 (dd, $J = 8.2$ and 2.2 Hz, 1H, H-6'), 3.70 (s, 3H, OCH₃), 3.47 (m, 1H, H-1'), 2.60–2.93 (m, 2H, H-3', H-3''), 1.86–2.04 (m, 2H, H-2', H-2''), 1.75 (s, 3H, CH₃CON⁻); FABMS (diastereomeric mixture of **29a,b**) (NBA; +ve) m/z 278 (M + H)⁺. Anal. (C₁₄H₁₈N₂O₃· $\frac{1}{4}$ H₂O) H, N: C: calcd for 62.90, found 63.37. The crystal structure of **29a** was solved by X-ray diffractometry as described below. **29b**: mp 207–210 °C; ¹H NMR (DMSO-*d*₆, 1 drop of DCl) δ 7.18 (d, $J = 8.3$ Hz, 1H, H-7'), 6.76 (br s, 1H, H-4'), 6.65 (br dd, $J = 8.3$ Hz, 1H, H-6'), 4.24 (d, $J = 8.4$ Hz, 1H, H-2), 3.69 (s, 3H, OCH₃), 3.31 (m, 1H, H-1'), 2.87 (m, 1H, H-3'), 2.71 (m, 1H, H-3''), 2.02 (m, 1H, H-2'), 1.90 (m, 1H, H-2''), 1.83 (s, 3H, CH₃CON⁻). Anal. (C₁₄H₁₈N₂O₃· $\frac{1}{4}$ H₂O), C, H, N.

(\pm)-rel-(1*R*,2*S*)-N^o-Acetyl-2-(5'-hydroxy-1'-indanyl)glycine Amide (30a). To a suspension of **29a** (130 mg, 0.5 mmol) in anhydrous CH₂Cl₂ (20 mL) was added BBr₃, 1.0 M in CH₂-Cl₂ (3.0 mL), and the suspension was stirred at room temperature (5 h). The reaction was quenched with MeOH (5 mL) and the mixture evaporated to dryness and then taken to

dryness again from MeOH (10 mL). The resulting foam was dissolved in MeOH (20 mL) and stirred (4 h) with 2 g of Dowex 50W-X4 strong cation exchange resin (50–100 mesh). The resin was filtered and washed with MeOH (10 mL), and the combined filtrates were taken to dryness, yielding crude **30a** quantitatively in sufficient purity for further use: $^1\text{H NMR}$ (DMSO- d_6) δ 7.81 (d, $J = 9.3$ Hz, 1H, NH), 7.25 (s, 1H, NH₂), 7.01 (s, 1H, NH₂), 6.90 (d, $J = 8.2$ Hz, 1H, H-7'), 6.57 (br s, 1H, H-4'), 6.48 (br dd, $^3J = 8.2$ Hz, 1H, H-6'), 4.62 (dd, $J = 9.1$ and 6.3 Hz, 1H, H-2), 3.42 (m, 1H, H-1'), 2.56–2.83 (2 m, H-3', H-3''), 1.78–2.06 (2 m, H-2', H-2''), 1.75 (s, 3H, CH₃CON⁻).

(±)-*rel*-(1'S,2S)-*N*^α-Acetyl-2-[5'-(hydroxy-1'-indanyl)glycine Amide (**30b**). A total of 100 mg (0.38 mmol) of **29b** was treated as described above for the preparation of **30a**, quantitatively yielding crude **30b** in sufficient purity for further use: $^1\text{H NMR}$ (DMSO- d_6 , 1 drop of D₂O) δ 7.06 (d, $J = 8.2$ Hz, 1H, H-7'), 6.58 (br s, 1H, H-4'), 6.48 (dd, $J = 8.2$ and 2.0 Hz, 1H, H-6'), 4.22 (d, $J = 8.5$ Hz, 1H, H-2), 3.27 (m, 1H, H-1'), 2.81 (m, 1H, H-3'), 2.63 (m, 1H, H-3''), 2.02 (m, 1H, H-2'), 1.84 (m, 1H, H-2''), 1.83 (s, 3H, CH₃CON⁻).

(±)-*rel*-(1'R,2S)-*N*^α-Acetyl-2-[5'-(O-phosphoro)-5'-hydroxy-1'-indanyl]glycine Amide (**3a**). To 0.5 mmol (theoretical yield) of crude **30a** and 1*H*-tetrazole (114 mg, 1.5 mmol) in anhydrous DMF (1 mL) was added di-*tert*-butyl *N,N*-diisopropylphosphoramidite (173 μL , 0.62 mmol), and the reaction mixture was stirred at room temperature (2.5 h). The mixture was briefly cooled to -78 °C, and then a solution of *m*-chloroperoxybenzoic acid (152 mg, 0.75 mmol) in anhydrous CH₂Cl₂ (1 mL) was added and the reaction continued at 0 °C (20 min). Solvent was removed at room temperature under high vacuum, and the residue was stirred with 90% aqueous TFA (5 mL; 1 h). The reaction mixture was taken to dryness under high vacuum and then re-evaporated from H₂O (5 mL). The residue was mixed with H₂O (5 mL), an insoluble solid was removed by filtration, and the filtrate was lyophilized. The resulting residue (497 mg) was purified by preparative HPLC [linear gradient from 10% B to 30% B over 30 min; solvent A = 0.05% TFA in H₂O; solvent B = 0.05% TFA in acetonitrile; H₂O (90:10); elution time, 8.4 min ($k' = 0.6$)], providing product **3a** as a white solid (96 mg), contaminated with diisopropylamine side product. The material was passed down a strong cation exchange column and repurified by HPLC to provide pure **3a** as a white solid (17 mg, 10% overall yield): $^1\text{H NMR}$ (DMSO- d_6) δ 7.88 (d, $J = 9.2$ Hz, 1H, NH), 7.42 (br s, 1H, NH₂), 6.97–7.12 (overlapping 2 br s, 1 d, NH₂, H-4', H-7'), 6.88 (br d, $J = 8.3$ Hz, 1H, H-6'), 4.7 (dd, $J = 9.2$ and 6.0 Hz, 1H, H-2), 3.48 (m, obscured by H₂O, 1H, H-1'), 2.62–2.96 (m, 2H, H-3', H-3''), 1.97 (m, 2H, H-2', H-2''), 1.76 (s, 3H, CH₃CON⁻); FABMS (Gly; ⁻ve) m/z 327 (M - H)⁻; HRMS calcd for C₁₅H₁₆N₂O₆P (M - H) 327.0746, found 327.0760.

(±)-*rel*-(1'S,2S)-*N*^α-Acetyl-2-[5'-(O-phosphoro)-5'-hydroxy-1'-indanyl]glycine Amide (**3b**). A total of 0.38 mmol (theoretical) of crude **30b** was treated as described above for the preparation of **3a** and purified in a similar manner (HPLC elution time 6.4 min ($k' = 0.2$) using a linear gradient of 10% B to 100% B over 30 min) to yield **3b** in 10% yield as a white solid: $^1\text{H NMR}$ (DMSO- d_6 , 500 MHz) δ 8.02 (d, $J = 9.1$ Hz, 1H, NH), 7.45 (s, 1H, NH₂), 7.20 (d, $J = 8.2$ Hz, 1H, H-7'), 7.06 (s, 1H, NH₂), 6.99 (s, 1H, H-4'), 6.85 (d, $J = 8.2$ Hz, 1H, H-6'), 4.31 (t, $J = 8.7$ Hz, 1H, H-2), 3.34 (m, 1H, H-1'), 2.88 (m, 1H, H-3'), 2.70 (m, 1H, H-3''), 2.06 (m, 1H, H-2'), 1.91 (m, 1H, H-2''), 1.83 (s, 3H, CH₃CON⁻); FABMS (Gly; ⁻ve) m/z 327 (M - H)⁻; HRMS calcd for C₁₅H₁₆N₂O₆P (M - H) 327.0746, found 327.0773.

Single Crystal X-ray Analysis of 10-HCl and 29a. Clear crystals of compound **20-HCl** and **29a** were selected for data collection in the θ/θ mode on a computer controlled automated diffractometer (Siemens R3m/V). Compound **29a** crystallized as a twin which was resolved by selecting a data crystal with major and minor components in a ratio greater than 3:1. The space group determinations were based on observation extinctions, E value statistics, and structure solutions. The data were corrected for Lorentz and polarization effects but not for absorption. Both structures were solved by direct methods with the aid of the program SHELXL⁴³ and refined by a full matrix least-squares⁴³ on F_o^2 . The refined parameters include

the coordinates and anisotropic thermal parameters for all non-hydrogen atoms. Carbon hydrogens used a riding model in which the coordinate shifts of the carbons were applied to the attached hydrogens with C-H = 0.96 Å, H angles idealized, and $U_{iso}(\text{H})$ set at fixed values. Experimental and structural analysis details, tables of crystal coordinates, and bond distances and bond angles are available as supplementary material. The absolute configuration of **20-HCl** was determined from the anomalous scattering from chlorine using the method of Flack.⁴⁴ The absolute structure parameter should be near zero with low ESD for the correct chirality and near 1 otherwise.

Molecular Modeling. Low-energy conformations of *N*^α-acetyl-L-tyrosine amide, benzazocine **10**, and indanylglycine **30a** were derived using molecular mechanics (CHARMm), semiempirical quantum mechanics AM1 and PM3 (MOPAC 6.0), and *ab initio* quantum mechanics with 6-31 or 6-31** basis sets (GAUSSIAN 92). In general, molecular mechanics were used to determine global energy minima via conformational searching. Precise energy minima conformations were then determined by semiempirical quantum mechanics and *ab initio* quantum mechanics.

SH2 Domain Binding Assays. Details of the SH2 domain competition assay have been published previously.⁴⁵ In this study six distinct assays were used to determine relative SH2 domain affinities for pTyr analogues versus high-affinity phosphopeptide ligands. In each assay a glutathione S-transferase (GST)/SH2 domain fusion protein was paired with an appropriate high-affinity [¹²⁵I]Bolton–Hunter radiolabeled phosphopeptide, and varying concentrations of unlabeled pTyr mimetics were added as competitors. The C-terminal SH2 domain of PI-3 kinase p85 was paired with IRS-1 pY628, GNGDpYMPMSPKS;⁴⁵ the Src SH2 domain was paired with hmT pY324, KEPQpYEEIPIYL;⁴⁶ the C-terminal SH2 domain of PLC γ was paired with PDGF pY1021, DNDpYIPLDPK;⁴⁵ the Lck SH2 domain was paired with the hmT pY324 sequence similar to assays conducted on the Src SH2 domain;⁴⁷ the Grb2 SH2 domain was paired with Shc pY317, ELFDDPSpYVN-VQNLDK;⁴⁷ and the N-terminal SH2 domain of SH-PTP2 was paired with IRS-1 pY1172, SLNpYIDLVLV.⁴⁸ An underline denotes the position of the [¹²⁵I]Bolton–Hunter modified lysine. GST/SH2 domain fusion proteins (0.5–1.0 μM , estimated by Bradford assay), 35 fmol of HPLC-purified [¹²⁵I]Bolton–Hunter-treated phosphopeptide (67 nCi), and varying concentrations of pTyr analogues were combined in 150 μL total volume of 20 mM Tris-HCl, 250 mM NaCl, 0.1% bovine serum albumin, and 10 mM dithiothreitol, pH 7.4, and vortexed. Glutathione–agarose (50 μL of a 1:10 buffered slurry; Molecular Probes) was added, and the samples were incubated overnight at 22 °C with constant mixing. Following centrifugation for 5 min at 12000g, supernatant solutions were removed by aspiration and [¹²⁵I] radioactivity associated with the unwashed pellets was determined with a γ -counter.

Acknowledgment. Appreciation is expressed to Ms. Pamela Russ and Dr. James Kelley of the LMC for mass spectral analysis. Supported in part by a grant to S.E.S. from the Council for Tobacco Research.

Supplementary Material Available: Tables of X-ray refinement parameters and atomic coordinates for compounds **10-HCl** and **29a** (6 pages). Ordering information is given on any current masthead page.

References

- (1) Brunton, V. G.; Workman, P. Cell-signaling targets for antitumor drug development. *Cancer Chemother. Pharmacol.* **1993**, *32*, 1–19.
- (2) Fry, M. J.; Panayotou, G.; Booker, G. W.; Waterfield, M. D. New insights into protein-tyrosine kinase receptor signaling complexes. *Protein Sci.* **1993**, *2*, 1785–1797.
- (3) Burke, T. R., Jr. Protein-tyrosine kinase inhibitors. *Drugs Future* **1992**, *17*, 119–131.

- (4) Brugge, J. S. New intracellular targets for therapeutic drug design. *Science* **1993**, *260*, 918–919.
- (5) Felder, S.; Zhou, M.; Hu, P.; Urena, J.; Ullrich, A.; Chaudhuri, M.; White, M.; Shoelson, S. E.; Schlessinger, J. SH2 domains exhibit high-affinity binding to tyrosine-phosphorylated peptides yet also exhibit rapid dissociation and exchange. *Mol. Cell. Biol.* **1993**, *13*, 1449–1455.
- (6) Songyang, Z.; Shoelson, S. E.; Chaudhuri, M.; Gish, G.; Pawson, T.; Haser, W. G.; King, F.; Roberts, T.; Ratnofsky, S.; Lechleider, R. J.; Neel, B. G.; Birge, R. B.; Fajardo, J. E.; Chou, M. M.; Hanafusa, H.; Schaffhausen, B.; Cantley, L. C. SH2 domains recognize specific phosphopeptide sequences. *Cell* **1993**, *72*, 767–778.
- (7) Booker, G. W.; Breeze, A. L.; Downing, A. K.; Panayotou, G.; Gout, I.; Waterfield, M. D.; Campbell, I. D. Structure of an SH2 Domain of the p85 alpha subunit of phosphatidylinositol-3-OH kinase. *Nature* **1992**, *358*, 684–687.
- (8) Overduin, M.; Rios, C. B.; Mayer, B. J.; Baltimore, D.; Cowburn, D. 3-Dimensional solution structure of the src homology-2 domain of c-abl. *Cell* **1992**, *70*, 697–704.
- (9) Waksman, G.; Kominos, D.; Robertson, S. C.; Pant, N.; Baltimore, D.; Birge, R. B.; Cowburn, D.; Hanafusa, H.; Mayer, B. J.; Overduin, M.; Resh, M. D.; Rios, C. B.; Silverman, L.; Kuriyan, J. Crystal structure of the phosphotyrosine recognition domain SH2 of v-src complexed with tyrosine-phosphorylated peptides. *Nature* **1992**, *358*, 646–653.
- (10) Eck, M. J.; Shoelson, S. E.; Harrison, S. C. Recognition of a high-affinity phosphotyrosyl peptide by the SRC homology-2 domain of p56(lck). *Nature* **1993**, *362*, 87–91.
- (11) Waksman, G.; Shoelson, S. E.; Pant, N.; Cowburn, D.; Kuriyan, J. Binding of a high affinity phosphotyrosyl peptide to the Src SH2 domain – Crystal structures of the complexed and peptide-free forms. *Cell* **1993**, *72*, 779–790.
- (12) Eck, M. J.; Atwell, S. K.; Shoelson, S. E.; Harrison, S. C. Structure of the regulatory domains of the SRC-family tyrosine kinase Lck. *Nature* **1994**, *368*, 764–769.
- (13) Hensmann, M.; Booker, G. W.; Panayotou, G.; Boyd, J.; Linacre, J.; Waterfield, M.; Campbell, I. D. Phosphopeptide binding to the N-terminal SH2 domain of the p85 alpha subunit of PI 3'-kinase: A heteronuclear NMR study. *Protein Sci.* **1994**, *3*, 1020–1030.
- (14) Lee, C. H.; Kominos, D.; Jacques, S.; Margolis, B.; Schlessinger, J.; Shoelson, S. E.; Kuriyan, J. Crystal structures of peptide complexes of the amino-terminal SH2 domain of the Syp tyrosine phosphatase. *Structure* **1994**, *2*, 423–438.
- (15) Pascal, S. M.; Singer, A. U.; Gish, G.; Yamazaki, T.; Shoelson, S. E.; Pawson, T.; Kay, L. E.; Forman-Kay, J. D. Nuclear magnetic resonance structure of an SH2 domain of phospholipase C-gamma 1 complexed with a high affinity binding peptide. *Cell* **1994**, *77*, 461–472.
- (16) Kuriyan, J.; Cowburn, D. Structures of SH2 and SH3 domains. *Curr. Opin. Struct. Biol.* **1993**, *3*, 828–837.
- (17) Waksman, G. Structural basis for peptide-binding specificity of SH2 domains. *Bull. Inst. Pasteur* **1994**, *92*, 19–25.
- (18) Giannis, A.; Kolter, T. Peptidomimetics for receptor ligands-discovery, development, and medical perspectives. *Angew. Chem., Int. Ed. Engl.* **1993**, *32*, 1244–1267.
- (19) Olson, G. L.; Bolin, D. R.; Bonner, M. P.; Bos, M.; Cook, C. M.; Fry, D. C.; Graves, B. J.; Hatada, M.; Hill, D. E.; Kahn, M.; Madison, V. S.; Rusiecki, V. K.; Sarabu, R.; Sepinwall, J.; Vincent, G. P.; Voss, M. E. Concepts and progress in the development of peptide mimetics. *J. Med. Chem.* **1993**, *36*, 3039–3049.
- (20) Greer, J.; Erickson, J. W.; Baldwin, J. J.; Varney, M. D. Applications of three-dimensional structures of protein target molecules in structure-based drug design. *J. Med. Chem.* **1994**, *37*, 1035–1054.
- (21) Moore, G. J. Designing peptide mimetics. *Trends Pharmacol. Sci.* **1994**, *15*, 124–129.
- (22) Appreciation is expressed to Dr. Michael Eck, Harvard Medical School, for providing Lck X-ray coordinates.
- (23) Nakatsuka, T.; Takashi, S.; Koyama, Y.; Ishiguro, M. Preparation of 2-(1-indanylglycine and related compounds). *Jpn. Kokai Tokkyo Koho* **1993**, Japanese Patent JP 05085999; *Chem. Abstr.* **1994**, *119*, 160844g.
- (24) Josien, H.; Lavielle, S.; Brunissen, A.; Saffroy, M.; Torrens, Y.; Beaujouan, J. C.; Glowinski, J.; Chassaing, G. Design and synthesis of side-chain conformationally restricted phenylalanines and their use for structure-activity studies on tachykinin NK-1 receptor. *J. Med. Chem.* **1994**, *37*, 1586–1601.
- (25) Perich, J. W.; Johns, R. B. Di-tert-butyl N,N-diethylphosphoramidite. A new phosphorylating agent for the efficient phosphorylation of alcohols. *Synthesis* **1988**, 142–144.
- (26) Shiotani, S.; Kometani, T. 9-Hydroxy-1,2,3,4,5,6-hexahydro-1,5-methano-3-benzazocine derivatives as analgesics. *J. Med. Chem.* **1977**, *20*, 310–312.
- (27) Murphy, J. G.; Ager, J. H.; May, E. L. Structures related to morphine. XIV. 2'-Hydroxy-5-methyl-2-phenethyl-6,7-benzomorphane, the 9-demethyl analog of NIH 7519 (phenazocine) from 3,4-dihydro-7-methoxy-2(1H)naphthalenone. *J. Org. Chem.* **1960**, *25*, 1386–1388.
- (28) Kidwell, R. L.; Darling, S. D. A facile phenol synthesis. An improved route to 6-methoxy-2-tetralone. *Tetrahedron Lett.* **1966**, *5*, 531–535.
- (29) Olofson, R. A.; Martz, J. T.; Senet, J.-P.; Piteau, M.; Malfroot, T. A new reagent for the selective, high-yield N-dealkylation of tertiary amines: Improved syntheses of naltrexone and nalbuphine. *J. Org. Chem.* **1984**, *49*, 2081–2082.
- (30) Rice, K. A. A rapid, high-yield conversion of codeine to morphine. *J. Med. Chem.* **1977**, *20*, 164–165.
- (31) Josien, H.; Chassaing, G. Asymmetric synthesis of the diastereomers of L-1-indanylglycine and L-1-benzylindanylglycine, χ_1, χ_2 -constrained side-chain derivatives of L-phenylalanine and L-2-naphthylalanine. *Tetrahedron Asymm.* **1992**, *3*, 1341–1354.
- (32) Evans, D. A.; Britton, T. C.; Ellman, J. A.; Dorow, R. L. The asymmetric synthesis of alpha-amino acids. Electrophilic azidation of chiral imide enolates, a practical approach to the synthesis of (R)- and (S)-alpha-azido carboxylic acids. *J. Am. Chem. Soc.* **1990**, *112*, 4011–4030.
- (33) Bergmann, E. D.; Solomonovici, A. Fulvenes and thermochromic ethylenes. Part 57. The Wittig-Horner reaction with fulvene ketones and related ketones. *Synthesis* **1970**, 183–189.
- (34) Gagnon, P. E.; Boivin, J. L.; Boivin, P. A. Synthesis of amino acids from substituted cyanoacetic esters. *Can. J. Res. Sect. B* **1950**, *28*, 207–212.
- (35) Basu, B.; Maity, S. K.; Mukherjee, D. Studies on intramolecular cyclizations. Synthesis of ring systems related to sesquiterpenoids. *Synth. Commun.* **1981**, *11*, 803–809.
- (36) Bax, A.; Freeman, R. Investigation of complex networks on spin-spin coupling by two-dimensional NMR. *J. Magn. Reson.* **1981**, *44*, 542–561.
- (37) QUANTA/CHARMm, a molecular modeling system, is supplied by Molecular Simulations, Inc., 200 Fifth Ave., Waltham, MA 01803-5279.
- (38) Stewart, J. J. P. MOPAC. Frank J. Seiler Research Laboratory, Air Force Academy: Boulder, CO 80840.
- (39) GAUSSIAN 92. Gaussian, Inc., Carnegie Office Park, Building 6, Pittsburgh, PA 15106.
- (40) Shoelson, S. E.; Sivaraja, M.; Williams, K. P.; Hu, P.; Schlessinger, J.; Weiss, M. A. Specific phosphopeptide binding regulates a conformational change in the PI 3-kinase SH2 domain associated with enzyme activation. *Embo J.* **1993**, *12*, 795–802.
- (41) Hoffommer, R. D.; Taub, D.; Wender, N. L. Structure of the Indenylacetic Acids. *J. Org. Chem.* **1969**, *34*, 4182–4184.
- (42) Papa, A. J. Synthesis and azidolysis of 2-chlorotetramethylguanidine. Synthetic utility of hexa- and tetramethylguanidinium azide. *J. Org. Chem.* **1966**, *31*, 1426–1430.
- (43) Sheldrick, G. M. *J. Appl. Crystallogr.*, in preparation.
- (44) Flack, H. D. On enantiomorph-polarity estimation. *Acta Crystallogr.* **1983**, *A39*, 876–881.
- (45) Piccione, E.; Case, R. D.; Domchek, S. M.; Hu, P.; Chaudhuri, M.; Backer, J. M.; Schlessinger, J.; Shoelson, S. E. Phosphatidylinositol 3-kinase p85 SH2 domain specificity defined by direct phosphopeptide/SH2 domain binding. *Biochemistry* **1993**, *32*, 3197–3202.
- (46) Payne, G.; Shoelson, S. E.; Gish, G. D.; Pawson, T.; Walsh, C. T. Kinetics of p56(lck) and p60(src) Src homology-2 domain binding to tyrosine-phosphorylated peptides determined by a competition assay or surface plasmon resonance. *Proc. Natl. Acad. Sci. U.S.A.* **1993**, *90*, 4902–4906.
- (47) Shoelson, S. E. Manuscript in preparation.
- (48) Case, R. D.; Piccione, E.; Wolf, G.; Bennett, A. M.; Lechleider, R. J.; Neel, B. G.; Shoelson, S. E. SH-Ptp2/Syp SH2 domain binding specificity is defined by direct interactions with platelet-derived growth factor beta-receptor, epidermal growth factor receptor, and insulin receptor substrate 1-derived phosphopeptides. *J. Biol. Chem.* **1994**, *269*, 10467–10474.

JM940755E